ISSN 1063-7850, Technical Physics Letters, 2016, Vol. 42, No. 2, pp. 113–117. © Pleiades Publishing, Ltd., 2016.
Original Russian Text © I.V. Borisenko, V.V. Demidov, A.A. Klimov, G.A. Ovsyannikov, K.I. Konstantinyan, S.A. Nikitov, V.L. Preobrazhenskii, N. Tiercelin, P. Pernod, 2016, published in Pis'ma v Zhurnal Tekhnicheskoi Fiziki, 2016, Vol. 42, No. 3, pp. 1–10.

Magnetic Interaction in the Manganite/Intermetallic Compound Heterostructure

I. V. Borisenko[a], V. V. Demidov[a], A. A. Klimov[a, b, d], G. A. Ovsyannikov[a], K. I. Konstantinyan[a], S. A. Nikitov[a], V. L. Preobrazhenskii[b, c], N. Tiercelin[b], and P. Pernod[b]

[a] *Kotel'nikov Institute of Radio Engineering and Electronics, Russian Academy of Sciences, Moscow, 125009 Russia*
[b] *International Associated Laboratory LEMAC-LICS: IEMN, UMR CNRS 8520, PRES Lille Nord de France, ECLille, 59651 Villeneuve d'Ascq, France*
[c] *Wave Research Center, Prokhorov Institute of General Physics, Russian Academy of Sciences, 119991 Russia*
[d] *Moscow State University of Information Technologies, Radio Engineering, and Electronics, Moscow, 119454 Russia*
e-mail: iboris@hitech.cplire.ru

Received September 3, 2015

Abstract—We investigate hybrid magnetic heterostructures consisting of thin epitaxial films of oxide ferromagnets $La_{0.7}Sr_{0.3}MnO_3$ and intermetallic superlattices $(TeCo_2/FeCo)_n$. The magnetic characteristics of the heterostructures were studied by the ferromagnetic resonance and magneto-optical Kerr effect techniques. The interlayer interaction in a heterostructure is shown to be antiferromagnetic. It was established that the interface with the intermetallic compound broadens the ferromagnetic resonance line of the manganite film.

DOI: 10.1134/S1063785016020048

The development of spintronic devices based on magnetically active materials with nanosized interfaces, tunnel magnetic contacts, devices with magnetoelectric interaction, et al., is an urgent problem that can be solved by clarifying the physical nature of structural and phase transformations in thin films and at the interfaces [1–5]. In divalent element-doped transition metal oxides $R_{1-x}A_xMnO_3$ (manganites), where R is La or Pr and A is Sr or Ca, new electron and magnetic phases can arise under the action of electric fields and stresses or at the interfaces with dielectrics or other oxides. Rare-earth intermetallic composites in the form of the exchange-coupled $TbCo_2$/FeCo nanolayers are characterized by giant magnetostriction, a high magnetomechanical coupling coefficient, controlled induced magnetic anisotropy, and spin-reorientation transitions induced by a magnetic field or elastic stresses [6–10].

The magnetic interaction and electron and spin states at the interface between the magnetic heterostructure layers determine both the magnetization reversal mechanisms and the spin-polarized current flow. This Letter presents the results of investigations of the magnetic interaction at the interfaces in heterostructures formed from the epitaxially grown manganite films with the composition $La_{0.7}Sr_{0.3}MnO_3$ (LSMO) and $(TeCo_2/FeCo)_n$ intermetallic superlattice (TCFC).

The LSMO epitaxial films were grown by laser ablation and magnetron sputtering at temperatures of 700–750°C and an oxygen pressure of 0.1–0.3 mbar. The used (110)$NdGaO_3$ (NGO) substrates ensured epitaxial growth of manganites. The orthorhombic structure of the NGO substrate provided dominance of the uniaxial magnetic anisotropy of the LSMO film in the substrate plane [11]. The intermetallic magnetic films were formed by sequential cathode sputtering of the $TeCo_2$ and FeCo layers in an additional magnetic field lying in the substrate plane and inducing uniaxial magnetic anisotropy of the obtained superlattices [6–9]. The magnetic anisotropy is determined by the value of an external magnetic field in the sputtering chamber. The heterostructures were formed so as to allow easy magnetization axes of the oxide and so that the intermetallic magnetic layers were parallel to one another. The TCFC superlattice was sputtered onto a (110)NGO substrate 5 × 5 × 0.5 mm in size with the epitaxial LSMO film through a 3-mm-square mask. This resulted in the formation of TCFC/LSMO heterostructure regions and free LSMO film regions on the NGO substrate.

The magnetic parameters of the heterostructure, including coercivity H_c, saturation field H_s, and magnetization M_s, were investigated using the meridional Kerr effect [11]. The magneto-optical setup for measuring the characteristics of the samples involved a semiconductor laser with $\lambda = 0.63$ μm and $P = 5$ μW, a light-dividing glass plate for forming reference and sig-

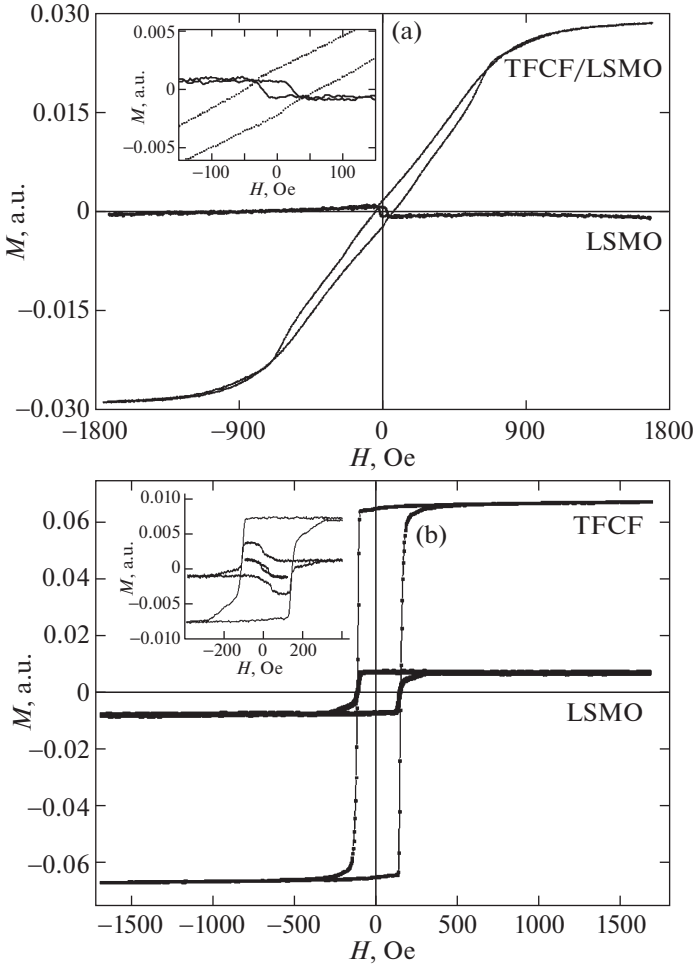

Fig. 1. Magnetization curves of the TCFC/LSMO heterostructure. The TCFC film thickness is 200 nm (n = 25). The LSMO film thickness is 30 nm. (a) The external magnetic field is directed along the hard magnetization axis. Inset: the enlarged central part of the plot. (b) The external magnetic field is directed along the easy magnetization axis; the magnetic field sweep range is ±2 kOe. Inset: the enlarged central part of the magnetization curve for the LSMO film for sweep ranges of ±100, ±400, and ±2 kOe.

nal beams, a half-wave phase plate for selecting the *s*- or *p*-type of polarization of the incident light, and a polarizer/analyzer for selecting the signal caused by the meridional Kerr effect. The investigated sample was placed on a rotary table in the electromagnet gap.

Figure 1 shows hysteresis loops for the TCFC/LSMO heterostructure with n = 25 (dashed line) upon focusing a 1-mm laser beam at the sample center. In the external magnetic field directed along the TCFC hard magnetization axis (Fig. 1a), the curve characteristic for rotation of the magnetic moment of the TCFC superlattice in the sample plane with a small (about 50 Oe) hysteresis was obtained. Saturation field $H_s \approx 1000$ Oe was much higher than H_s of the LSMO film, which is indicative of the dominant effect of the TCFC superlattice on the hysteresis loop of the structure. The effect of magnetism of the lower LSMO film was not observed, which is apparently related to screening of the laser beam by the TCFC film. Upon focusing of the laser beam at the sample place where the TCFC superlattice is missing, the magnetization changes its sign, which is apparently due to the antiferromagnetic ordering of the TCFC and LSMO layers.

Figure 1b shows hysteresis loops measured in the field directed along the easy axis. The coercivity of the TCFC superlattice was 140 Oe. Upon focusing of the laser beam on the LSMO film, the hysteresis loop is determined by the magnetic field variation amplitude. In the narrow range of magnetic field sweep, the hysteresis loop of the LSMO film changes its sign, as in the magnetic field directed along the hard axis, and the hysteresis loop width is approximately equal to the coercivity of the LSMO film (see the inset to Fig. 1a). At a field amplitude of more than 400 Oe, the magnetization curve for the LSMO film repeats the shape of the hysteresis loop of the TCFC superlattice. Since the preliminary (before TCFC sputtering) measurements of the LSMO hysteresis loop yielded small values

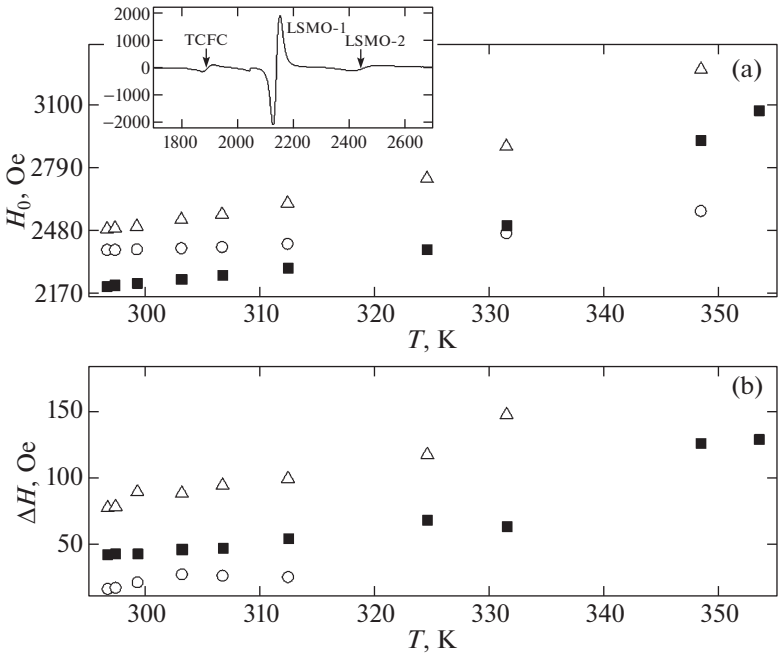

Fig. 2. Temperature dependences of the parameters of the films obtained using FMR. (a) Resonance fields H_0 and (b) resonance linewidths ΔH. Open triangles and closed squares correspond to the LSMO film; circles correspond to the TCFC film. Inset: room-temperature FMR spectrum of the TCFC/LSMO heterostructure obtained in the external magnetic field directed along the easy magnetization axis. The amplitude of the low-field TCFC line is ten times larger than for the two other lines.

$H_c = 10$ Oe, the results presented in Fig. 1 evidence magnetic interaction between the LSMO and TCFC films; however, the character of this interaction is difficult to establish because of the distance between the points of hysteresis measurements in the layers.

The character of the magnetic interaction between the films in the heterostructure can be determined using ferromagnetic resonance (FMR). The ferromagnetic resonance spectra were studied on an ER 200 standard magnetic resonance spectrometer (Bruker) operating in the 3-cm microwave range. Angular and temperature dependences of resonance field H_0 and width ΔH of the FMR lines were investigated in the dc magnetic field and magnetic component of the microwave field directed perpendicular to each other and remaining in the film plane during substrate rotation (the so-called parallel orientation). The substrate was rotated around the axis perpendicular to the film plane. This technique prevents signal variation caused by shape anisotropy and is suitable for studying only the planar anisotropy. Ferromagnetic resonance field H_0 is related to the resonance frequency by the equation containing the magnetization and anisotropy fields with different symmetry as parameters [12].

Figure 2 shows temperature dependences of H_0 and ΔH for the three spectral lines observed in the heterostructure. The spectrum presented in the inset to Fig. 2 was detected at room temperature and frequency $\omega/2\pi = 9.74$ GHz. The dc magnetic field was directed parallel to the easy magnetization plane. It can be seen in the inset to Fig. 2 that there are three ferromagnetically ordered spin subsystems. The temperature dependences of H_0 for the detected lines show (Fig. 2a) that the low-field FMR line corresponds to the Curie temperature above 360 K and belongs to the TCFC film sputtered onto the LSMO film, while the two other lines belong to the LSMO films. The numbers of spins in both subsystems belonging to the LSMO film (the estimation was carried out by comparing the areas of absorption lines) are comparable, similar to the squares of these film parts. One of these subsystems may be associated with the spins belonging to the LSMO film part that lies directly under the TCFC film square (LSMO-1) and the other, with the spins of the rest part of the film (LSMO-2). Linewidths ΔH measured between the peaks of the absorption line derivative in these parts of the LSMO film differ by 40–50 Oe. Since these parts of the LSMO film are located on one substrate and have identical crystal quality, the differences in ΔH values are most likely related to the interaction between TCFC and LSMO. Such an FMR line broadening in the ferromagnet–normal metal system was observed earlier and theoretically described in [13] as a consequence of the purely spin current leakage from the ferromagnet to the metal.

Figure 3 shows the room-temperature angular dependence of resonance fields for the three observed spin subsystems. It can be seen that the resonance

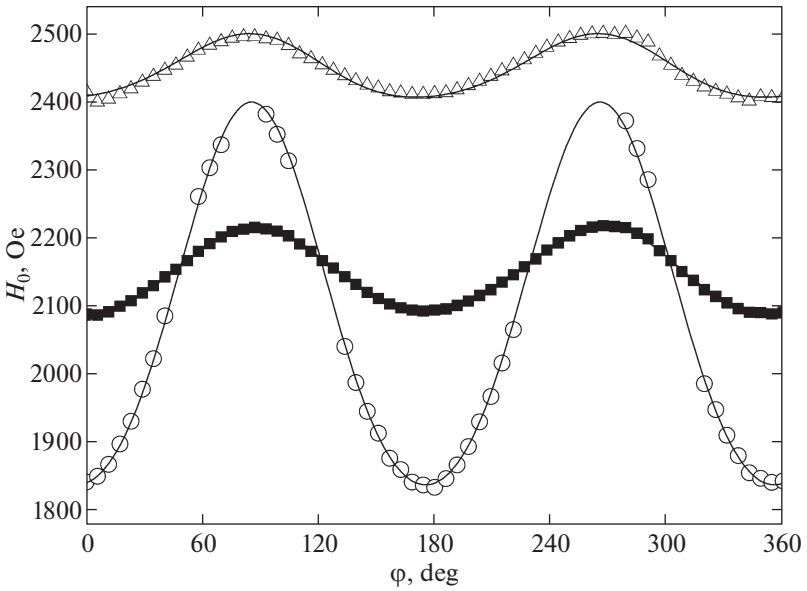

Fig. 3. Angular dependence of the resonance fields for the three FMR lines of the TCFC/LSMO heterostructure. Solid lines show the calculated dependences. Triangles and rectangles correspond to the LSMO film; circles correspond to the TCFC film.

fields of the spin subsystems in the heterostructure change in a magnetic field range greatly0 exceeding the magnetization range (Fig. 1). Consequently, in the magnetic field range of the FMR measurements (inset to Fig. 2), all the spin subsystems in the structure saturate and all magnetic moments are directed along the external magnetic field. For LSMO-2, the resonance ratio obtained in [14] can be used:

$$\left(\frac{\omega}{\gamma}\right)^2 = (H_0 + H_u\cos 2\varphi_u + H_c\cos 4\varphi_c) \times\left(4\pi M_0 + H_0 + H_u\cos^2\varphi_u + H_c\frac{1+\cos^2 2\varphi_c}{2}\right). \quad (1)$$

Here, γ is the gyromagnetic ratio, $H_u = 2K_u/M_0$ and $H_c = 2K_c/M_0$ are the fields of the uniaxial planar anisotropy and biaxial cubic anisotropy with corresponding constants K_u and K_c, φ_u and φ_c are the angles between the uniaxial anisotropy and biaxial cubic anisotropy easy axes and the external magnetic field, M_s is the equilibrium magnetization, and H_0 is the resonance magnetic field.

It can be seen in Fig. 3 that the easy axes in all three spin subsystems (the minimum value of H_0) are almost parallel (the axes' rotation is no more than 2°–3°). The two upper dependences (triangles and squares in Fig. 3) correspond to the two LSMO subsystems. The dependence with the lower resonance fields describes the behavior of the FMR line corresponding to the LSMO-1 film part, since the parameters of this line (width and resonance field) are characteristic of the LSMO film on the NGO substrate. To describe the FMR line corresponding to LSMO-2, one should take into account the interlayer exchange between the two ferromagnetically ordered layers, LSMO and TCFC. In other words, it is necessary to consider the free energy of the united spin system of the LSMO-2 and TCFC films that are in contact, which consists of the Zeeman interaction energies and the magnetic anisotropy with the corresponding constants, and to take into account the bilinear exchange with constant J. In this case, the magnetizations of these films are assumed to be uniform over the volume. Note that the interlayer exchange energies are proportional to the squares of the contacting surfaces and the Zeeman and anisotropy energies are proportional to the layer volume [15].

The solution of the Landau–Lifshitz–Gilbert equation yields the two resonance relations describing the FMR in the TCFC and LSMO-2 layers. These relations are analogous to expression (1), but the H_0 value should be replaced by the sums of two terms $H_{01} + H_{J1}$ and $H_{02} + H_{J2}$ for the LSMO-2 and TCFC layers, respectively. Here, $H_{J1} = J/(M_1d_1)$ and $H_{J2} = J/(M_2d_2)$ are the effective interlayer exchange fields for the LSMO-2 and TCF layers, respectively, and d_1 and d_2 are the thicknesses of these layers.

The angular dependences obtained from the resonance relations for the LSMO-2 and TCFC layers, which describe best the experimental data, are shown in Fig. 3 by solid lines. First, the calculated line for the single LSMO-1 film was built. Then, using the obtained magnetization of the LSMO layer and the resonance relation under the interlayer exchange conditions, the calculated curve for the LSMO-2 film was built. This allowed interlayer exchange value J to be determined. Finally, using the obtained J value, the calculated curve for the TCFC film was constructed,

which allowed the M_2 value to be obtained. As a result, we may state that, in the investigated TCFC/LSMO structure grown on the NGO substrate, the interlayer exchange interaction with the negative constant $J = -0.24$ erg/cm is implemented, which causes the antiferromagnetic character of this interaction.

Acknowledgements. We are grateful to V.A. Atsarkin, Yu.V. Kislinskii, and A.V. Shadrin for help in the experiments and useful discussion.

This study was supported by the Russian Academy of Sciences, the Russian Foundation for Basic Research (projects nos. 14-02-00165, 14-07-00258, and 14-07-93105), and a Grant of the President of the Russian Federation for Support of Leading Scientific Schools NSh-4871.2014.2.

REFERENCES

1. E. Dagotto, Science **309**, 257 (2005).
2. J. Mannhart, in *Thin Films and Heterostructures for Oxide Electronics*, Ed. by S. Ogale (Springer, New York, 2005), p. 251.
3. C. H. Ahn, et al., Rev. Mod. Phys. **78**, 1185 (2006).
4. S. M. Wu, Shane A. Cybart, P. Yu, M. D. Rossell, J. Zhang, et al., Nat. Mater **9**, 756 (2010).
5. K. I. Konstantinyan, Yu. V. Kislinskii, G. A. Ovsyannikov, A. V. Shadrin, A. E. Sheierman, A. L. Vasil'ev, M. Yu. Presnyakov, and F. V. Komissinskii, Phys. Solid State **55** (3), 461 (2013).
6. H. Le Gall, J. Ben Youssef, F. Socha, N. Tiercelin, V. Preobrazhensky, and P. Pernod, J. Appl. Phys. **87** (9), 5783 (2000).
7. E. Quandt, A. Ludwig, D. G. Lord, and C. A. Faunce, J. Appl. Phys. **83**, 7267 (1998).
8. N. Tiercelin, V. Preobrazhensky, P. Pernod, H. Le Gall, and J. Ben Youssef, J. Magn. Magn. Mater. **210**, 302 (2000).
9. N. Tiercelin, V. Preobrazhensky, P. Pernod, and A. Ostachenko, Appl. Phys. Lett. **92**, 062 904 (2008).
10. Y. Dusch, V. Rudenko, N. Tiercelin, S. Giordano, V. Preobrazhensky, and P. Pernod, Nanomater. Nanostruct. **2**, 44 (2012).
11. G. A. Ovsyannikov, A. M. Petrzhik, I. V. Borisenko, A. A. Klimov, Yu. A. Ignatov, V. V. Demidov, and S. A. Nikitov, JETP **108**, 48(2009).
12. V. V. Demidov, G. A. Ovsyannikov, A. M. Petrzhik, I. V. Borisenko, A. V. Shadrin, and R. Gunnarsson, J. Appl. Phys. **113**, 163 909 (2013).
13. Y. Tserkovnyak and A. Brataas, Phys. Rev. Lett. **88**, 117 601 (2002).
14. V. V. Demidov, I. V. Borisenko, A. A. Klimov, G. A. Ovsyannikov, A. M. Petrzhik, and S. A. Nikitov, JETP **112** (5), 825 (2011).
15. A. B. Drovosekov, O. V. Zhotikova, N. M. Kreines, et al., JETP **89** (5), 986 (1999).

Translated by E. Bondareva

SPELL:OK